

Dispersive dynamics of photoexcitations in conjugated polymers measured by photomodulation spectroscopy

O. Epshtein,^{1,2} G. Nakhmanovich,³ Y. Eichen,^{1,3} and E. Ehrenfreund^{1,2}

¹*Solid State Institute, Technion, Israel Institute of Technology, Haifa 32000, Israel*

²*Department of Physics, Technion, Israel Institute of Technology, Haifa 32000, Israel*

³*Department of Chemistry, Technion, Israel Institute of Technology, Haifa 32000, Israel*

(Received 24 October 2000; published 12 March 2001)

We study the dynamics of the long-lived photoexcitations in *p*-phenylene-vinylene based conjugated polymers containing acid-sensitive bipyridine subunits, and in *poly*(5,5'-vinylene-2,2'-bipyridylene), by following the dependence of the intensity of the photoinduced absorption bands on the laser modulation frequency. The photoinduced absorption spectra contain two broad bands, whose relative intensities strongly depend on the protonation state of the polymers and whose modulation frequency dependence is distinctly different. Whereas the higher-energy band follows the modulation frequency dependence expected for either mono- or bimolecular recombination process, the lower-energy band shows a fractional power law frequency dependence at high modulation frequencies, strongly indicating a “dispersive relaxation” process. The value of the fractional exponent is sample dependent and is a quantitative measure for the distribution of the relaxing centers.

DOI: 10.1103/PhysRevB.63.125206

PACS number(s): 78.66.Qn, 78.40.Me, 77.84.Jd, 73.50.Gr

I. INTRODUCTION

Photoinduced absorption (PIA) spectroscopy has served as a useful tool for investigating the nature of the photogenerated species in conjugated polymers.^{1–3} Time dependent PIA studies have been instrumental in revealing the excitation and recombination processes of the photocarriers.⁴ The dynamics of the long-lived photoexcitations can be very conveniently studied by following their dependence on the modulation frequency of the exciting laser pump. For example, in *poly*(2,5-dimethoxy-*p*-phenylene vinylene),⁵ two types of long time dynamics were observed. Triplet excitons were found to obey a monomolecular recombination process, where the falloff of the magnitude of the PIA absorbance, $|\Delta T/T|$, with increasing modulation frequency, ω , follows a ω^{-1} behavior at high frequencies. On the other hand, bipolarons showed a much slower falloff of the magnitude of the PIA absorbance: $\omega^{-0.4}$ at high frequencies. Another example is polyaniline, where the pernigraniline and emeraldine forms show different frequency behavior. Whereas for pernigraniline the two PIA bands show a similar falloff, in emeraldine base the two bands behave differently: $\omega^{-(0.5-0.6)}$ and $\omega^{-0.2}$, respectively.^{6,7} The different modulation frequency behavior verified the different origin of the two photoexcited species. Similarly, polarons in sexi-thiophene films⁸ revealed also a slow falloff of the PIA absorbance with ω . The gentle frequency dependence was interpreted as due to a spread in recombination rates in the inhomogeneous samples.^{5,8} In oligomers based on thiophene units,⁹ both mono- and bimolecular recombination mechanisms were found for triplet excitons.

Distribution profiles of relaxation times have been widely used to describe relaxation processes in amorphous and glassy materials.^{10–12} The description of the complex relaxation processes in these materials required the use of special distribution functions. Experimental data in these materials were commonly interpreted in terms of the Kohlrausch–

Williams–Watts (KWW) function, the so-called “stretched exponential” decay,^{10,12,13}

$$\phi(t) = \exp[-(t/\tau_K)^\beta], \quad (1)$$

where $0 < \beta < 1$ and τ_K is the KWW time constant. The mechanisms leading to the stretched exponential behavior have been broadly discussed in the literature.^{10,13} For example, it may describe diffusive (or dispersive) charge relaxation in amorphous solids containing high density of electronic traps.¹³ The exponent β was shown¹³ to be determined by the effective dimensionality of the configuration relaxation space. Furthermore, the stretched exponential relaxation is closely related to a broader family of dispersive relaxation processes, such as Cole–Cole¹⁴ or Havriliak–Negami,¹⁵ in which the response to a modulated excitation depends on a fractional power of the modulation frequency, ω .^{12,16} The lifetime distribution functions for all these mechanisms were calculated and are summarized elsewhere.¹⁷ One of the common features to all the dispersive processes is the, relatively gentle, high frequency falloff of the response: $\omega^{-\alpha}$, with $\alpha < 1$.¹¹

In the present work we follow the dynamics of photoexcitations in bipyridine-PPV derivatives by measuring the PIA dependence on the modulation frequency on a wide frequency range. We find an evidence for a “dispersive dynamics” characterized by unusually slow falloff of the PIA at high modulation frequencies. We show that the dispersive nature can be quantified as a monomolecular (or bimolecular) recombination process augmented by an asymmetric lifetime distribution having an appreciable contribution at short lifetimes. In addition, we connect this dispersive behavior with a stretched exponential relaxation in the time domain.

The π -conjugated polymers studied here are optically tunable derivatives of pyridylene/vinylene polymers. Recently, we have shown¹⁸ that these derivatives can be tuned reversibly via protonation–deprotonation (P–DP) processes. Considerable luminescence red shifts (up to 0.2 eV) were

observed upon exposing free-base films to acid vapors. Films of the free-base form showed, in general, sharper spectra than the corresponding protonated films, due to increased disorder in the latter. The PIA spectra of the two forms revealed two types of photoexcited species, whose density or absorption intensity depend on the protonation state of the polymer.

II. EXPERIMENTAL

As was discussed in our earlier study,¹⁸ the tunability of the photo- and electrophysical properties of the polymers originates probably from structural (intra- and interstrand) changes associated with the protonation–deprotonation processes and aggregation of the strands. In the present report, we deal with the free-base (“pristine”) form of the polymers and its fully protonated (i.e., acid-saturated) form, obtained after exposing it to HCl vapors. Thin films for optical measurements were prepared by drop casting on glass or quartz substrates from formic acid solutions. The free-base films were obtained by heating the films in vacuum (10^{-5} mmHg) to above 70 C for over 12 h.

The photoinduced absorption (PIA) spectra were obtained by recording the negative relative differential transmission, $-\Delta T/T$, due to the application of modulated optical beam.¹⁸ The modulated signal is measured using a lock-in technique in which both the in-phase (IP) and out-of-phase (OP) components are obtained. Since the lock-in measures only the first harmonics at frequency ν , we write for simplicity the fully modulated excitation beam as

$$g(t) = (g/2) \times (1 + \cos \omega t), \quad (2)$$

where $\omega = 2\pi\nu$ and g is proportional to the pump intensity. If $S(t)$ is the time dependent system response following the application of $g(t)$, then the measured IP and OP components are given by

$$S_{IP} = \int_{\text{period}} S(t) \cos(\omega t) dt, \quad (3)$$

$$S_{OP} = \int_{\text{period}} S(t) \sin(\omega t) dt.$$

The IP and OP components thus yield complementary information regarding the recombination mechanisms and characteristic lifetime, τ , of the photoexcitations.

For simple mono- or bimolecular recombination processes, the IP component is a monotonic decreasing function of the modulation frequency and it reduces to half its zero frequency value at approximately $\omega_{\text{max}} = (\tau)^{-1}$. At this frequency the OP component, being zero at zero modulation frequency, reaches its maximum value.¹⁹ The behavior of the IP and OP components in more realistic recombination processes is discussed in Sec. IV A 1 in more details.

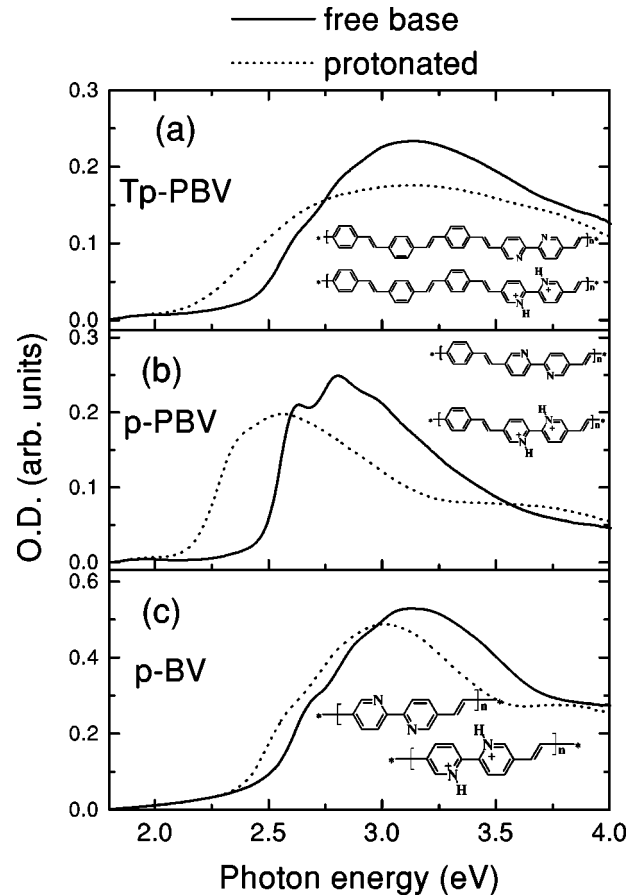


FIG. 1. The optical absorption spectra of Tp-PBV (a), p-PBV (b), and p-BV (c) films in their free-base (solid line) and protonated (dotted line) forms. The chemical structures shown in (a)–(c) are for the free-base (top) and protonated (bottom) forms of each of the films.

III. EXPERIMENTAL RESULTS

Figure 1 shows the absorption spectra of films of all three polymers both in their free-base (solid lines) and fully protonated (dotted lines) forms. The respective molecular structure of the free-base (top) and protonated (bottom) polymers are given as inserts to Fig. 1. Consider first the absorption spectra of p-PBV [Fig. 1(b)]. It is seen that the free-base spectrum is sharper than that of the protonated films. In the free-base form, the vibronic structure is apparent, whereas in the protonated form the spectrum is much broader and it is red shifted by about 0.2 eV. The broader spectrum indicates different morphology, which is more inhomogeneous than the morphology of the free-base form. This issue was discussed in detail in previous publications.^{18,20} Similar behavior is observed for the other two polymers Tp-PBV and p-BV [Figs. 1(a) and 1(c), respectively]: the protonated forms appear to be less ordered than the free-base films.

Figure 2 shows the PIA spectra of films of all three polymers both in their free-base (solid lines) and fully protonated (dotted) lines forms. Both the free-base and protonated polymer spectra contain two bands: a low-energy (LE) band and a high-energy (HE) band. However, the two PIA spectra are very distinct from each other. Consider first the PIA spectra

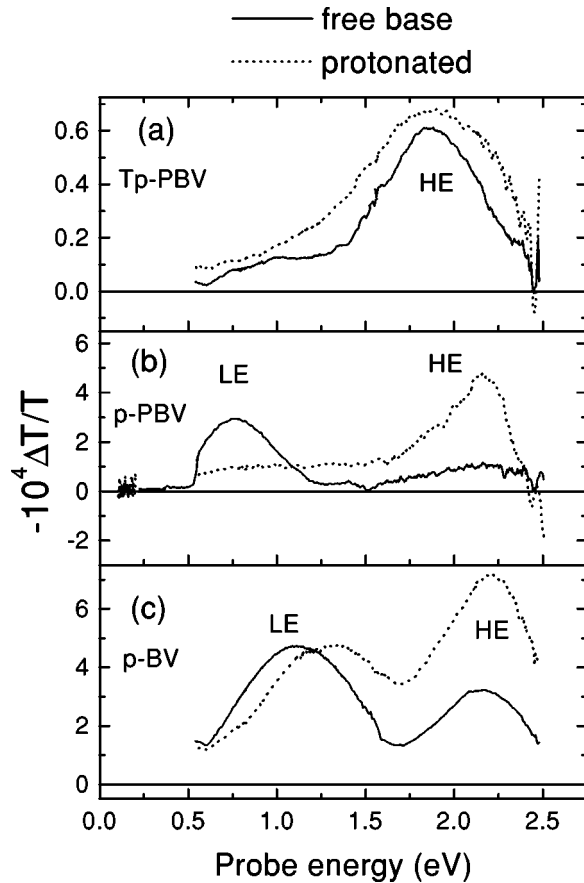


FIG. 2. The PIA spectra for Tp-PBV (a), p-PBV (b), and p-BV (c) films in their free-base (solid line) and protonated (dotted line) forms. The HE and LE bands are marked.

of p-PBV [Fig. 2(b)]. In the free-base film, the LE band (peak position at ≈ 0.8 eV) is much stronger than the HE band (peak position at ≈ 2.2 eV), while in the protonated film, the relative intensities are reversed. It is then implied that the two bands have a different origin. Note that no absorption due to photoinduced infrared active vibrations (IRAV), characteristic of charged polarons, were observed both for free-base and protonated samples. The missing IRAV lines indicate that the LE and HE bands originate from optical transitions due to neutral photoexcited species, such as (triplet) excitons. It is seen that in the less ordered morphology, the HE band is dominant, while in the more ordered, free-base morphology, the LE band is more dominant. It is thus plausible to assume that the LE band originates at intrachain triplet transitions, while the HE band is due to interchain excitons which are affected by aggregation. Similar, but not identical, behavior is apparent also in Tp-PBV. Starting from the protonated form, the HE band weakens as the film becomes less protonated, but stays quite strong even in the free-base films. The broader absorption spectra and the larger HE intensity in the PIA spectra are indicative of a less-order morphology in Tp-PBV. In p-BV, the differences between the free-base and protonated forms are less distinguished.

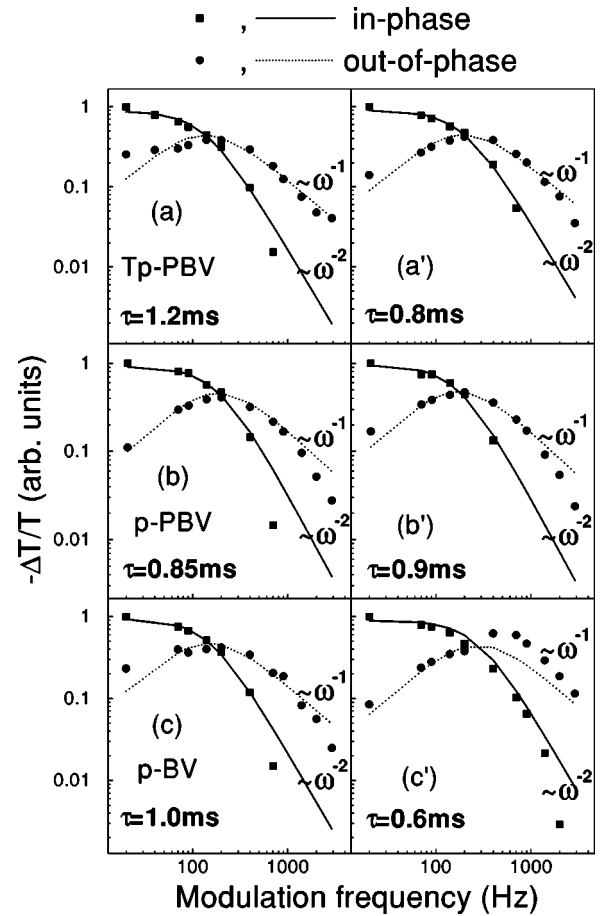


FIG. 3. The modulation frequency dependence of the HE band shown in Fig. 2. Solid square (circle) symbols represent the in-phase (out of phase) data. The lines are fits to monomolecular recombination processes Eq. (5). Similar fits were obtained for a bimolecular mechanism. Note the log–log scale.

Our main interest is the characterization of the recombination dynamics corresponding to the long lived photoexcitations responsible for the HE and LE bands. To that end, we have measured the modulation frequency dependence of the two bands, which can yield direct indication for the recombination processes and characteristic lifetimes.¹⁹ In Fig. 3, we show the modulation frequency dependence of the HE band for the two forms of all three polymers. It shows the characteristic behavior expected for both the IP and OP components. The OP component (Fig. 3, solid circles) reaches its maximum at frequency ν_{\max} (in the range of 130–260 Hz for all samples) where the IP component (Fig. 3, solid squares) reduces to half of its zero frequency value. This value of ν_{\max} indicates a characteristic lifetime of $\tau = (2\pi\nu_{\max})^{-1}$ in the range 0.6–1.2 ms (as marked in Fig. 3), for the defects responsible for the HE transition. At higher modulation frequencies, $\omega \equiv 2\pi\nu > 2\pi\nu_{\max}$, both the IP and OP components decrease as a power law: $\omega^{-\beta}$, with $\beta=2$ and 1, respectively. This is the expected behavior for either mono- or bimolecular recombination mechanism (see below Sec. IV A 1).

The LE band behaves quite differently with respect to the modulation frequency, as shown in Fig. 4 for p-PBV and

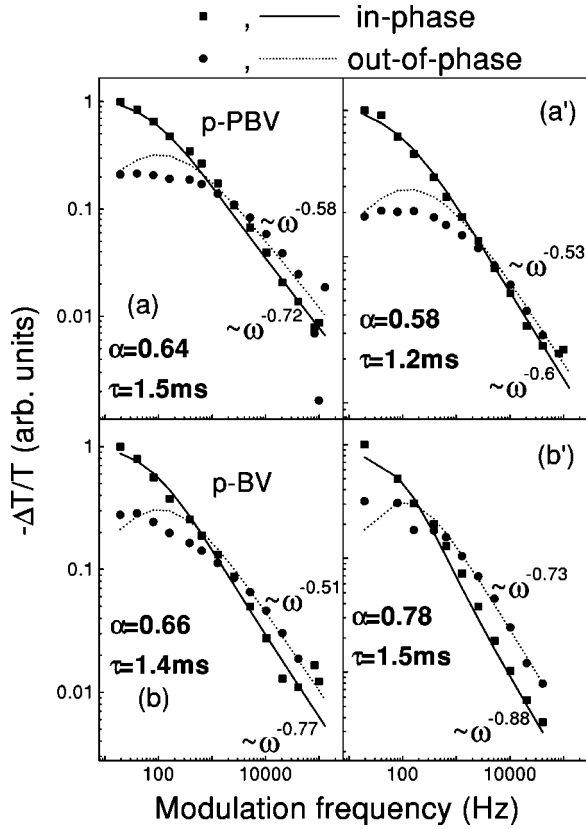


FIG. 4. The modulation frequency dependence of the LE band shown in Fig. 2. Solid square (circle) symbols represent the in-phase (out of phase) experimental data. The lines are fits to the dispersive relaxation process [Eq. (6)]. Note the log–log scale.

p-BV (the LE band in Tp-PBV is too weak for such detailed measurements). Comparing Figs. 3 and 4, we observe three main differences in the modulation frequency dependence between the LE and HE bands. (a) The maximum of the OP component in LE is much less apparent than in HE. (b) The IP component in LE does not level off at low ω as in HE. (c) At high frequencies, both IP and OP components of LE decrease very gently, as $\omega^{-\gamma}$ with $\gamma < 1$ (as marked in Fig. 4), compared with the much stronger dependence for HE (see Fig. 3). These differences strongly indicate a wide distribution of recombination lifetimes. We will show below that the peculiar high frequency dependence of the PIA LE band can naturally be explained by “dispersive” (or diffusive) recombination processes.

We have also measured the laser intensity dependence of both the HE and LE bands. In all films, the PIA bands are sublinear with the laser intensity reaching near saturation at high intensities. This tendency towards saturation results most probably due to traps that limit the recombination as they become saturated. The PIA temperature dependence also indicates trap limited recombination processes with finite activation energy. In the presence of saturable traps, both mono- and bimolecular processes would result in a sub-linear dependence on the pump intensity. We therefore did not attempt to determine the recombination mechanism using the laser intensity dependence of the PIA.

IV. DISCUSSION

A. Recombination kinetics

1. Frequency response

The photomodulation method applied in this work is a very convenient tool by which one can follow the frequency response of the photoexcited system over a wide dynamic range (0.1 Hz–1 MHz). The PIA signal, at either the HE or LE absorption band, is a direct measure of the density, ρ , of photoexcited species responsible for the respective electronic transitions. Therefore, the lock-in response $S(t)$ [Eq. (3)] is proportional to ρ . Denoting by U the carrier recombination rate, we can write the rate equation for the photoexcited species as

$$\frac{d\rho}{dt} = g(t) - U\rho, \quad (4)$$

where g is defined in Eq. (2). For example, in a monomolecular recombination process characterized by lifetime τ , $U = \rho/\tau$, and the system frequency response is then

$$\begin{aligned} \rho_{IP}(\omega) &= g\tau/(1 + \omega^2\tau^2), \\ \rho_{OP}(\omega) &= g\omega\tau^2/(1 + \omega^2\tau^2). \end{aligned} \quad (5)$$

We see that at $\omega = \omega_{\max} \equiv (\tau)^{-1}$, ρ_{OP} has a maximum and $\rho_{IP} = \rho_{OP}$. At higher frequencies, $\omega > \omega_{\max}$, $\rho_{IP} < \rho_{OP}$. The asymptotic behavior, for each of the components, is a power law decrease: $\omega^{-\beta}$, where $\beta = 2$ and 1 , for the IP and OP components, respectively. This dependence on the frequency is characteristic not only to monomolecular recombination process, but also to bimolecular processes and their combination. Furthermore, assuming a finite-width Gaussian (or Lorentzian) distribution of recombination rates does not significantly change this frequency dependence.

Since films of conjugated polymers, in general, and ours in particular, are very inhomogeneous at the molecular level, they resemble amorphous materials. The dynamics of photoexcitations in amorphous materials is governed in many cases by a “dispersive” (or diffusive) process.^{10,14} In a dispersive process, the response, $R(\omega)$, of the system to a modulated excitation depends nontrivially on a fractional power of the (modulation) frequency, ω .^{11,14} For the sake of simplicity, we consider the simplest nontrivial mechanism found in amorphous materials,¹⁴

$$R(\omega) = \frac{R_0}{1 + (i\omega\tau_0)^\alpha}, \quad (6)$$

where $\alpha < 1$, τ_0 is a “mean” lifetime, and R_0 is the steady-state response at zero frequency. In Eq. (6), the PIA response, R , is written as a complex function whose real (imaginary) part is the IP (OP) component. The response $R(\omega)$ in Eq. (6) is originally assigned to the dielectric response of the system.^{11,14} Here, we use it to evaluate the density of the photogenerated species undergoing relaxation/recombination processes following a modulated photoexcitation at frequency ω . We therefore identify R_0 in Eq. (6) as the steady-state photoexcitation density at zero frequency.

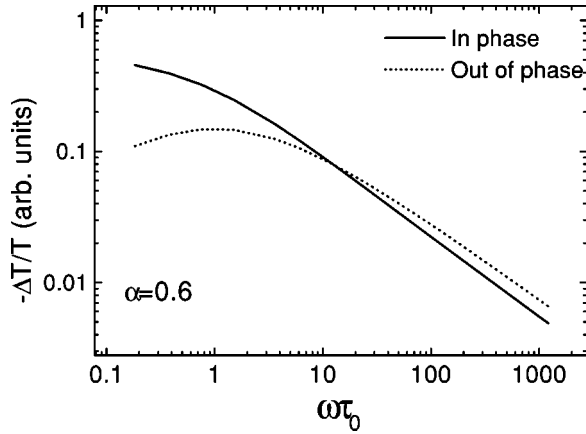


FIG. 5. The expected frequency dependence of the PIA for the dispersive process Eq. (6) for $\alpha=0.6$. Note the log–log scale.

Quite generally, R_0 can be written as $R_0 = g\tau_0$, where g is the photogeneration rate, which is proportional to the excitation intensity and the quantum efficiency and should include some averaging over lifetime distribution (see below). In Fig. 5 we show the expected frequency response for a dispersive recombination process, with $\alpha=0.6$. It is seen that (a) the OP component still maintains a maximum at $\omega \approx \tau_0^{-1}$; and (b) at higher frequencies, both the OP and IP components decrease as $\omega^{-\beta}$, where β_{OP} is slightly higher than α and β_{IP} is slightly lower than α .

2. Lifetime distributions for dispersive processes

It was shown previously^{12,16,17} that the empirical dispersive dielectric response functions in the frequency domain [e.g., Eq. (6), as a representative example] can be described in terms of Debye relaxation augmented by lifetime distribution. Following Ref. 17 we define the lifetime distribution function $\Gamma(\ln \tau)$ by the equation

$$R(\omega) = \int_{-\infty}^{\infty} \frac{R_0(\tau)}{1 + i\omega\tau} \Gamma(\ln \tau) d \ln(\tau), \quad (7)$$

where $R(\omega)$ is given by Eq. (6). In Eq. (7), $R_0(\tau)$ is the zero frequency steady-state photoexcitation density for a given lifetime τ : $R_0(\tau) \equiv g\tau$. The dispersive process is thus described as a single lifetime recombination combined with a lifetime distribution function $\Gamma(\ln \tau)$. The single lifetime process may, for instance, be a monomolecular process or a bimolecular process, for which τ depends on the excitation intensity. This distribution function Γ can be extracted from the measured response $R(\omega)$, using the inverse transform of Eq. (7).¹⁷ Thus, measuring the PIA as a function of the modulation frequency, can yield the inhomogeneous distribution of recombination lifetimes.

B. Analysis of PIA frequency response

The PIA modulation frequency dependence of the LE band, Fig. 4, indicates a dispersive recombination mechanism, since the high-frequency falloff is very slow: $\omega^{-\alpha}$ ($\alpha \approx 0.5-0.7$). We have thus used Eq. (6) to fit the IP

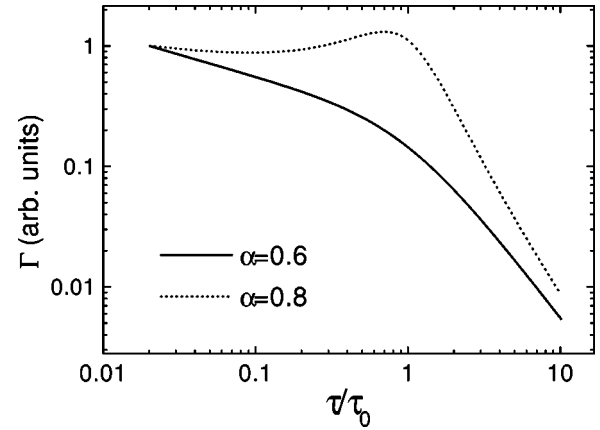


FIG. 6. The distribution function $\Gamma(\tau)$ for the dispersive process Eq. (7) for $\alpha=0.6$ and 0.8 . Note the log–log scale.

and OP components of the LE band. The results of the fit are shown in Fig. 4 as solid and dashed lines, respectively, along with the values of α obtained by these fits. The different values of α are possibly associated with the amorphous nature of the different films. The smaller value of α found for the protonated form indicates more disorder in accordance with earlier measurements.^{18,20} The very good fits support the assumption of a dispersive mechanism for the photocarrier dynamics.²¹

As mentioned in Sec. IV A 2 above, the frequency response of the PIA, $R(\omega)$, can be described in terms of mono- (or bi-) molecular relaxation combined with a distribution, $\Gamma(\ln \tau)$, of primitive relaxation times, τ . The distribution function Γ can be easily realized once α in Eq. (6) is obtained experimentally. In Fig. 6 we show the lifetime distribution function $\Gamma(\ln \tau)$ obtained using Eq. (7), for two representative values: $\alpha=0.6$ and 0.8 . It is seen that Γ thus obtained is asymmetric with respect to τ_0 , having an appreciable long tail at short relaxation times. We conjecture that it is this short relaxation times tail that is responsible for the gentle high frequency falloff characterized by $\alpha < 1$. It means also that there is an appreciable amount of photoexcited species that diffuse very fast between traps.

Finally, it is of interest to connect the dispersive exponent α [Eq. (6)] with the KWW exponent, β [Eq. (1)]. Each of these two exponents gives rise to a certain distribution of primitive lifetimes.^{12,17} By comparing the resulting distribution functions, one can arrive at interrelation between the two exponents.¹⁶ Using the relation given in Fig. 3 of Ref. 16, we find for each value of α the corresponding value of β . These are listed in Table I. The exponent β is related to the effective dimensionality, \tilde{d} , of the configuration space in which the relaxation takes place:¹³

$$\beta = \tilde{d}/(\tilde{d} + 2). \quad (8)$$

Simple, unconstrained, diffusion in three dimensions corresponds to $\tilde{d}=3$ and $\beta=0.6$. Diffusion under constraints due to short and/or long range forces gives rise to ‘‘fractal’’ dimensionality, resulting in $\tilde{d} < 3$ and $\beta < 0.6$. The results summarized in Table I indicate that the dispersive relaxation pro-

TABLE I. The dispersive parameters for the LE band in the various films: **1.** p-PBV free-base; **2.** p-PBV protonated; **3.** p-BV free-base; and **4.** p-BV protonated. α and τ_0 are extracted from the fits of Fig. 4, β is the KWW exponent, and \tilde{d} is the effective dimensionality, calculated using Eq. (8).

	α	$\tau_0(\text{ms})$	β	\tilde{d}
1	0.64 ± 0.06	1.5 ± 0.2	0.51 ± 0.06	2.1 ± 0.4
2	0.58 ± 0.06	1.2 ± 0.2	0.46 ± 0.06	1.7 ± 0.4
3	0.66 ± 0.06	1.4 ± 0.2	0.54 ± 0.06	2.3 ± 0.5
4	0.78 ± 0.07	1.5 ± 0.2	0.67 ± 0.01	4 ± 1

cess in our films takes place in a fractal configuration space with effective dimensionality $\tilde{d} \leq 3$.

V. CONCLUSIONS

We have studied the long-time dynamics of photoexcited species in bipyridine/PPV derivatives using frequency dependent photomodulation spectroscopy. We have shown that

“dispersive” relaxation is the dominant mechanism in cases where the high frequency falloff is slow. We have invoked an empirical expression for the frequency dependent photo-induced response function, analogous to the “dispersive transport” expressions, used commonly in amorphous substances. We have successfully accounted for the fractional power frequency dependence and have found the appropriate distribution of relaxation times that equivalently describes the fractional power behavior. In addition, we have shown that our analysis can be connected to a relaxation process described by a stretched exponential behavior.

We add in passing that it is highly conceivable that the fractional power-law dependence reported previously for other polymers and oligomers (e.g., Refs. 5 and 8) can similarly be accounted for by the “dispersive” relaxation mechanism.

ACKNOWLEDGMENTS

This work was supported by the U.S.-Israel Binational Science Foundation (BSF), and by the Israeli Ministry of Science.

- ¹J. Orenstein, Z. Vardeny, G. L. Baker, G. Eagle, and S. Etemad, Phys. Rev. B **30**, 786 (1985).
- ²Z. Vardeny, E. Ehrenfreund, O. Brafman, M. Nowak, H. Schaffer, A. J. Heeger, and F. Wudl, Phys. Rev. Lett. **56**, 671 (1986).
- ³K. E. Ziemelis, A. T. Hussain, D. D. C. Bradley, R. H. Friend, J. R u he, and G. Wagner, Phys. Rev. Lett. **66**, 2231 (1991).
- ⁴Z. Vardeny and E. Ehrenfreund, in *Transport and Relaxation Processes in Random Materials*, edited by J. Klafter, R. J. Rubin, and M. F. Shlesinger (World Scientific, Singapore, 1986), p. 127.
- ⁵H. S. Woo, S. C. Graham, D. A. Halliday, D. D. C. Bradley, R. H. Friend, P. L. Burn, and A. B. Holmes, Phys. Rev. B **46**, 7379 (1992).
- ⁶M. G. Roe, J. M. Ginder, P. E. Wigen, A. J. Epstein, M. Angelopoulos, and A. G. MacDiarmid, Phys. Rev. Lett. **60**, 2789 (1988).
- ⁷N. S. Sariciftci, L. Smilowitz, Y. Cao, and A. J. Heeger, J. Chem. Phys. **98**, 2664 (1993).
- ⁸J. Poplawski, E. Ehrenfreund, J. Cornil, J. L. Br edas, R. Pugh, M. Ibrahim, and A. J. Frank, Mol. Cryst. Liq. Cryst. A **256**, 407 (1994).
- ⁹R. A. J. Janssen, L. Smilowitz, N. S. Sariciftci, and D. Moses, J. Chem. Phys. **101**, 1787 (1994).

- ¹⁰G. Pfister and H. Scher, Adv. Phys. **27**, 747 (1978).
- ¹¹K. L. Ngai and C. T. White, Phys. Rev. B **20**, 2475 (1979).
- ¹²F. Alvarez, A. Algeria, and J. Colmenero, Phys. Rev. B **4**, 7306 (1991).
- ¹³J. C. Phillips, Rep. Prog. Phys. **59**, 1133 (1996); Chem. Phys. **212**, 41 (1996).
- ¹⁴K. S. Cole and R. H. Cole, J. Chem. Phys. **9**, 341 (1941).
- ¹⁵S. Havriliak, Jr. and S. Negami, J. Polym. Sci., Part C: Polym. Symp. **14**, 99 (1966).
- ¹⁶F. Alvarez, A. Algeria, and J. Colmenero, Phys. Rev. B **47**, 125 (1993).
- ¹⁷A. Bello, E. Laredo, and M. Grimaud, Phys. Rev. B **60**, 12764 (1999).
- ¹⁸Y. Eichen, G. Nakhmanovich, V. Gorelik, O. Epshtein, J. M. Poplawski, and E. Ehrenfreund, J. Am. Chem. Soc. **120**, 10463 (1998).
- ¹⁹E. Dekel, E. Ehrenfreund, D. Gershoni, P. Boucaud, I. Sagnes, and Y. Campidelli, Phys. Rev. B **56**, 15734 (1997).
- ²⁰G. Nakhmanovich, O. Epshtein, V. Gorelik, J. M. Poplawski, J. Oiknine-Schlesinger, E. Ehrenfreund, and Y. Eichen, Synth. Met. **101**, 269 (1999).
- ²¹See also D. Epshtein, G. Nakhmanovich, Y. Eichen, and E. Ehrenfreund, Synth. Metals (to be published).